Nanoscale

PAPER

Surface-confined fluorescence enhancement of Au nanoclusters anchoring to a two-dimensional ultrathin nanosheet toward bioimaging†

Cite this: *Nanoscale*, 2016, 8, 9815

Rui Tian, Dongpeng Yan, Chunyang Li, Simin Xu, Ruizheng Liang,* Lingyan Guo, Min Wei,* David G. Evans and Xue Duan

Gold nanoclusters (Au NCs) as ultrasmall uorescent nanomaterials possess discrete electronic energy and unique physicochemical properties, but su er from relatively low quantum yield (QY) which severely a ects their application in displays and imaging. To solve this conundrum and obtain highly-e cient uorescent emission, 2D exfoliated layered double hydroxide (ELDH) nanosheets were employed to localize Au NCs with a density as high as 5.44×10^{13} cm^{-2}, by virtue of the surface con nement e ect of ELDH. Both experimental studies and computational simulations testify that the excited electrons of Au NCs are strongly con ned by MgAl-ELDH nanosheets, which results in a largely promoted QY as well as prolonged uorescence lifetime (both ~7 times enhancement). In addition, the as-fabricated Au NC/ELDH hybrid material exhibits excellent imaging properties with good stability and biocompatibility in the intracellular environment. Therefore, this work provides a facile strategy to achieve highly luminescent Au NCs *via* surface-con ned emission enhancement imposed by ultrathin inorganic nanosheets, which can be potentially used in bio-imaging and cell labelling.

Received 26th February 2016,
Accepted 12th April 2016

DOI: 10.1039/c6nr01624c

www.rsc.org/nanoscale

Introduction

Metal nanoclusters (NCs) are ultrasmall nanoparticles (usually less than 2 nm) comprised of several to hundred atoms, which show discrete energy levels, molecule-like electronic transitions and resulting unique physicochemical properties.[1,2] Compared with traditional chromophores (e.g., quantum dots (QDs) with obvious toxicity, organic molecules with poor stability),[3] metal NCs such as Au NCs possess the advantages of low toxicity, high solubility, large Stokes shifts, excellent chemical and photo-stability,

electron–hole recombination would result in an improved QY.

[12] Previous studies have shown that the coating of inorganic nanocrystals by a shell material with a larger band gap is an e ective method to realize the localization of excitons and the resulting enhanced QY.[13] Although a 3D spacial confinement has been explored, an emission enhancement from a surface confinement e ect imposed by a 2D matrix is not revealed.

Layered double hydroxides (LDHs) are a class of 2D inorganic layered materials with diversity in chemical composition and structural morphology.[14] By virtue of a liquid exfoliation strategy, LDH microcrystals can be exfoliated into

State Key Laboratory of Chemical Resource Engineering, Beijing University of Chemical Technology, Beijing 100029, China. E-mail: liangruizheng2000@163.com, weimin@mail.buct.edu.cn; Fax: +86-10-64425358; Tel: +86-10-64412131

†Electronic supplementary information (ESI) available. See DOI: 10.1039/c6nr01624c

This journal is © The Royal Society of Chemistry 2016

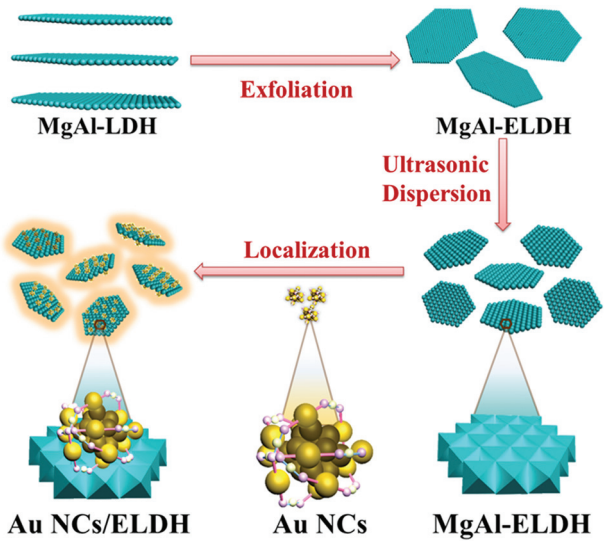

Scheme 1 Schematic representation for the fabrication of the Au NC/ELDH hybrid material.

positively-charged monolayer nanosheets that serve as a building block or substrate.[15] Previously, we prepared a Au NC/LDH film via a layer-by-layer self-assembly technique, and found that the interlaminar confinement significantly enhances the fluorescence emissive Au(I) content owing to the host–guest electrostatic interaction.[15b] This inspires us to further explore whether a surface confinement e ect of an exfoliated LDH nanosheet (ELDH) would boost the fluorescence emission of Au NCs. According to the band gap theory, if the forbidden zone of ELDH can be tuned to cover that of Au NCs, an intrinsic localization of excitons from Au NCs will be achieved and an enhanced emission will be obtained. In this work, Au NCs (~2 nm) are localized onto the surface of MgAl-ELDH nanosheets with an extremely high density (denoted as Au NCs/ELDH, Scheme 1). As expected, the excited electrons of Au NCs are restricted by the MgAl-ELDH nanosheets, which results in markedly depressed electron mobility and extremely enhanced QY (from 2.60% to 19.05%). Density functional theory plus Hubbard correction (DFT+U) calculations were performed to study the band gap of Au NCs and various LDHs, and the results show that MgAl-ELDH nanosheets can e ectively confine the excited electrons and facilitate the electron–hole recombination, in accordance with the experimental results. In addition, the bio-imaging performance of the Au NC/ELDH hybrid material is demonstrated, and the excellent photostability, anti-photobleaching properties as well as good biocompatibility would guarantee its potential application.

Results and discussion

Structural and morphological characterization

Au NCs were synthesized similar to the previous work with some modifications.[8a–c] Briefly, glutathione and hydrogen tetrachloroaurate hydrate were mixed and hydrothermally treated at 70 °C for 24 h. Due to the existence of a glutathione ligand, the obtained Au NCs are negatively-charged with a zeta potential of −7.21 mV (Fig. 1A, red curve). The hydrodynamic diameter of Au NCs is distributed in the range 2–4 nm by dynamic light scattering (DLS) measurements (Fig. 1B, red column); The TEM image shows a particle size of ~2 nm with a high monodispersion (Fig. S1†). The ultrathin ELDH nanosheets with a lateral size of ~100 nm were obtained via exfoliation of MgAl-LDH microcrystals followed by vigorous ultrasonic dispersion. Subsequently, Au NCs were anchored onto MgAl-ELDH nanosheets by a thorough blending followed by centrifugation and redispersion in water (see the ESI† for details). Due to the interaction between Au NCs and ELDH (electrostatic force and hydrogen bonding), the Au NC/ELDH nanohybrid remains stable in the aqueous solution within three months (Fig. S2†). The obtained Au $NC_x/ELDH_y$ (x/y stands for the ratio of Au NCs to ELDH) nanohybrids exhibit positive electricity with a zeta potential in the range 30.7–49.4 mV (Fig. S3 and Table S1†); a typical sample of Au $NCs_3/ELDH_1$ with 33.8 mV is illustrated in Fig. 1A (green curve). The hydrodynamic diameter of the Au NC/ELDH nanohybrid ranges from 60–160 nm according to DLS measurements (Fig. 1B, green; Fig. S4 and Table S1†), which is suitable for cell uptake through clathrin-mediated endocytosis according to the previous report.[16] TEM images (Fig. S5†) of Au $NC_x/ELDH_y$ samples show an increasingly enhanced loading density of Au NCs along with the increase of the x/y ratio. Typical TEM images of Au $NCs_3/ELDH_1$ (marked by green dash) are shown in Fig. 1C–E, from which numerous Au NCs (the black dots circled in red dash) are immobilized onto the surface of lamellar ELDH homogeneously and uniformly. The loading density as high as 5.44×10^{13} cm^{-2} was calculated by counting the number of supported Au NCs in a selected ELDH surface area via the TEM image (Fig. 1C–E and S6†). Moreover, the loading content of Au NCs for Au $NC_x/ELDH_y$ samples was also determined by inductively coupled plasma atomic

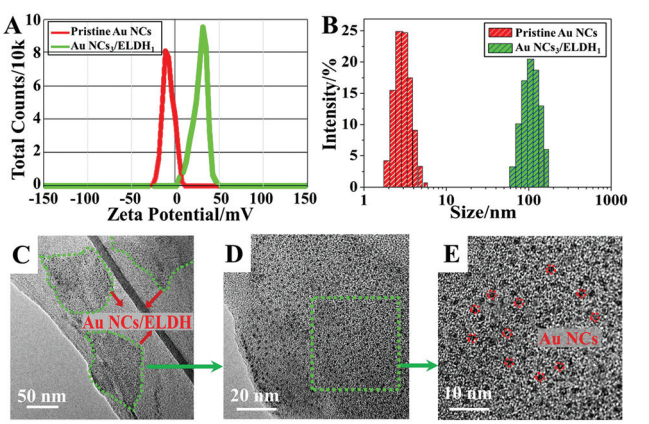

Fig. 1 (A) Zeta potential and (B) size distribution of pristine Au NCs (red) and the Au $NC_3/ELDH_1$ hybrid material (green). (C, D, E) TEM images of Au $NCs_3/ELDH_1$ at different magnifications.

This journal is © The Royal Society of Chemistry 2016

emission spectroscopy (ICP-AES). The molar ratio of localized Au NCs to ELDH enhances from 0.42 to 3.17 as the x/y value increases from 0.5 to 4 (Table S2†). In addition, as the molar ratio of Mg/Al in ELDH increases from 2 to 4, the density of localized Au NCs reduces obviously (Fig. S7†), which can be ascribed to the decreased positive charge density of ELDH.[17]

Fluorescence studies

Photoluminescence properties of pristine Au NCs and Au NC/ELDH samples were systematically investigated. As shown in Fig. 2A (line 10), the pristine Au NCs exhibit a weak emission at ~566 nm (orange color) under UV light radiation (Fig. 2B, Sample 10); while ELDH nanosheets are nonluminous (Fig. 2A: line 1, and Fig. 2B: sample 1). In contrast, the Au NC_x/$ELDH_y$ samples show a blue shift of ~6 nm, which may result from the surface confinement e ect imposed by LDH nanosheets (e.g., depressed interactions between adjacent Au–Au or Au–solvent molecules).[18] The fluorescence intensity of Au NCs/ELDH enhances gradually along with the increase of x/y from 0.5 : 1 to 3 : 1 and then decreases from 3 : 1 to 4 : 1 (Fig. 2A, line 2 to 9). This can be further testified by the photographs of these samples under UV irradiation (Fig. 2B) with the same quantity of Au NCs. Relative QYs are also calculated for Au NCs_x/$ELDH_y$ (x/y = 0–4, Table S3†). With the enhancement of the x/y ratio, the QY of Au NC_x/$ELDH_y$ nanohybrids increases at first to a maximum and then decreases; the highest QY (19.05%) is observed for Au NCs_3/$ELDH_1$, which is ~7.3 folds to that of the pristine Au NCs (2.60%). The increment of QY as large as 7.08 times is also confirmed by the absolute fluorescence QY, indicating the significant promotion of fluorescence e ciency in the Au NC_3/$ELDH_1$ composite. Moreover, The QY of Au NCs_3/$ELDH_1$ decreases from 19.05% to 14.33% with the increment of the Mg/Al ratio from 2 to 4 (Table S4 and Fig. S8†).

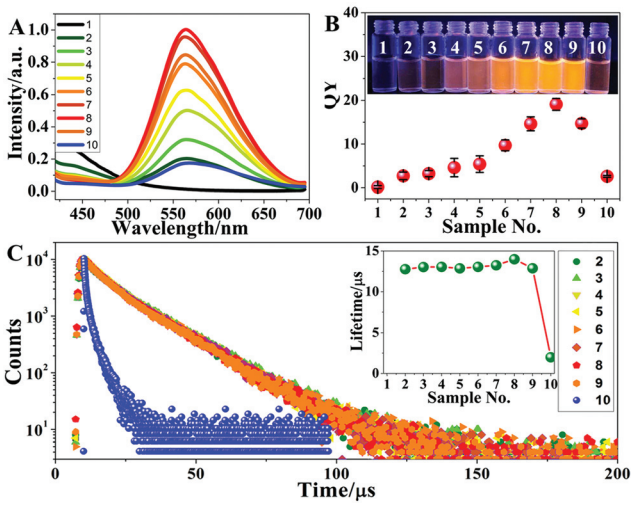

Fig. 2 (A) Fluorescence spectra, (B) relative QY, and (C) fluorescence decay curves of Au NCs_x/$ELDH_y$ with various x/y ratios under the conditions of equivalent Au contents (from Sample 1 to 10): x/y = 0 : 1, 0.5 : 1, 0.75 : 1, 1 : 1, 1.25 : 1, 1.5 : 1, 2 : 1, 3 : 1, 4 : 1 and 1 : 0, respectively. The inset in B shows sample photographs under UV light radiation (365 nm).

The excitation-state lifetime of Au NCs before and after immobilization onto ELDH nanosheets was further studied. The average fluorescence lifetime of aqueous pristine Au NC solution is ~1.99 μs (Fig. 2C and Table S5†); while it is boosted largely in the case of Au NC_x/$ELDH_y$ samples. For Au NCs_3/$ELDH_1$, the lifetime is ~13.99 μs (Fig. 2C and Table S5†), which is 7 times longer than that of pristine Au NCs. The prolonged lifetime accompanied by enhanced QY could be attributed to the confinement e ect by the host–guest interaction, which inhibits the non-radiation transition after Au NCs are tightly anchored onto ELDH nanosheets. This will be further discussed in the following section.

X-ray photoelectron spectroscopy (XPS) has been employed as an e ective technique to study the relationship between the valence state and fluorescence properties of Au NCs before and after localization by ELDH nanosheets.[10,11] As illustrated in Fig. S9A† (curve a), the binding energy of pristine Au NCs (blue line) is located at 84.2 eV, which is between that of the Au(I)–thiol portion (red line: 84.7 eV) and Au(0) nanocrystals (green line: 83.8 eV). The content of fluorescent emissive component Au(I)–thiol is determined to constitute ~34.5% in pristine Au NCs. In contrast, after the incorporation with ELDH nanosheets, this value increases to 49.8% (Fig. S9B†, curve e). Moreover, the binding energy of Au in Au NCs/ELDH shifts to 84.5 eV (Au(I) shifts from 84.7 to 85.1 eV), which can be ascribed to the electrostatic attraction and polarization e ect of positively-charged ELDH nanosheets.

To further reveal the influence of the ELDH support on the valence state change of Au NCs, various carrier materials including montmorillonoid (MMT, electronegative), graphene oxide (GO, electronegative), poly-diallyldimethylammonium chloride (PDDA, electropositive) as well as ELDH with di erent metallic compositions (CoAl-ELDH and CoNi-ELDH, electropositive) were used as supports for the immobilization of Au NCs. The corresponding TEM images of these composites are shown in Fig. S10.† Compared with pristine Au NCs, both the peak position and relative content of Au(I) do not show obvious change for the samples of Au NCs/MMT, Au NCs/PDDA and Au NCs/GO (the relative content of Au(I) ranges from 33.0–35.3%, Fig. S9A†) while this value enhances to 47.2% and 48.1% for Au NCs/CoAl-ELDH and Au NCs/CoNi-ELDH, respectively, close to Au NCs/MgAl-ELDH (49.8%) studied above (Fig. S9B†). The results indicate that no obvious polarization e ect is found between Au NCs and MMT, PDDA or GO while ELDH with di erent metal cations can promote the relative content of Au(I) due to the electropositivity of ELDH nanosheets.

The corresponding fluorescence emission spectra and lifetime decay curves of these samples were also studied. In comparison with Au NCs, no variation in fluorescence intensity is observed for Au NCs/MMT and Au NCs/PDDA and the fluorescence quenching of Au NCs/GO occurs due to the fast electron transfer between Au NCs and GO as reported previously (Fig. S11 and Tables S6, S7†).[19] Thus, MMT, PDDA and GO are

not suitable substrates to optimize the emission of Au NCs. Interestingly, in the cases of Au NC/X-ELDH (X = MgAl, CoAl and CoNi) samples, although the relative contents of Au(I) in these samples are similar, their fluorescence performances are rather di erent. As shown in Fig. 3A, the fluorescence intensity of Au NCs/MgAl-ELDH is much stronger than the other two ELDH supports; the QY values follow the tendency: Au NCs/MgAl-ELDH (19.05%) ≫ Au NCs/CoAl-ELDH (4.85%) > Au NCs/CoNi-ELDH (4.71%) (Table S6†). Moreover, the lifetime of Au NCs/MgAl-ELDH is much longer than that of Au NCs/CoAl-ELDH and Au NCs/CoNi-ELDH (Table S7† and Fig. 3C). The di erent fluorescence properties of Au NCs/X-ELDH (X = MgAl, CoAl and CoNi) enlighten us that the relative content of fluorescent Au(I) is not the crucial factor which determines the largely improved QY and lifetime. Further study is needed to reveal the intrinsic mechanism.

According to the principles of fluorescence QY, boosting the recombination of electrons and holes is one e ective way to improve the luminescence QY. If the excited electrons are e ectively confined by a matrix with a broad band gap, a promoted radiation transition and enhanced QY will be obtained.[13] In order to testify whether the excitons of Au NCs can be localized by ELDH nanosheets, we investigate the electron mobility of pristine Au NCs and Au NC/X-ELDH (X = MgAl, CoAl and CoNi) nanohybrids. The Nyquist plot of the electrochemical impedance spectroscopy (EIS) is a useful method to study the charge transfer resistance, which provides information on electron mobility.[20] EIS was thus employed to study the electron confinement e ect of Au NCs induced by di erent ELDH substrates. The results in Fig. 3B show that the electron mobility decreases as follows: Au NCs/CoNi-ELDH > Au NCs/CoAl-ELDH > Au NCs > Au NCs/MgAl-ELDH. In other words, MgAl-ELDH possesses the best electron confinement ability and the excited electrons/holes of Au NCs can be localized by MgAl-ELDH nanosheets, which facilitate the recombination of electrons/holes and thus promotes fluorescence performances (intensity, QY and lifetime). Therefore, MgAl-ELDH nanosheets serve as excellent substrates which impose a surface confinement e ect toward excitons, giving rise to a largely enhanced fluorescence emission.

In order to further verify the electron confinement e ect of the LDH matrix, density functional theory plus Hubbard correction (DFT+U) calculations were carried out to study the band edge placements of Au NCs, MgAl-LDH, CoAl-LDH and CoNi-LDH (see the ESI† for detailed calculations). For non-periodic Au NCs, the HOMO and LUMO are calculated to be −5.221 eV and −3.181 eV, respectively. For periodic MgAl-LDH, CoAl-LDH and CoNi-LDH, the conduction band minimum (E_{CBM}) and valence band maximum (E_{VBM}) are obtained by their band structure and work function (Fig. 4A–C and S12†). The E_{VBM} values of MgAl-LDH, CoAl-LDH and CoNi-LDH are calculated to be −5.275 eV, −6.123 eV and −5.783 eV while the E_{CBM} values are −0.701 eV, −3.739 eV and −4.700 eV, respectively (shown in Fig. 4D). By comparing the E_{CBM} of Au NCs with these LDH samples, the excited electron of Au NCs can transfer to the conduction band of CoAl-LDH and CoNi-LDH rather than MgAl-LDH. Therefore, it is concluded that only the MgAl-LDH matrix can provide a confined microenvironment for excited electrons of Au NCs, which facilitates the recombination of electrons/holes. In addition, the molecular dynamics simulations of Au NCs/MgAl-ELDH, Au NCs/CoAl-ELDH and Au NCs/CoNi-ELDH were carried out. As shown in Fig. 4E–G, the geometries of Au NCs (Fig. S13†) are optimized with the glutathione ligand attaching to the surface of the LDH nanosheet. The binding energy values between Au NCs and

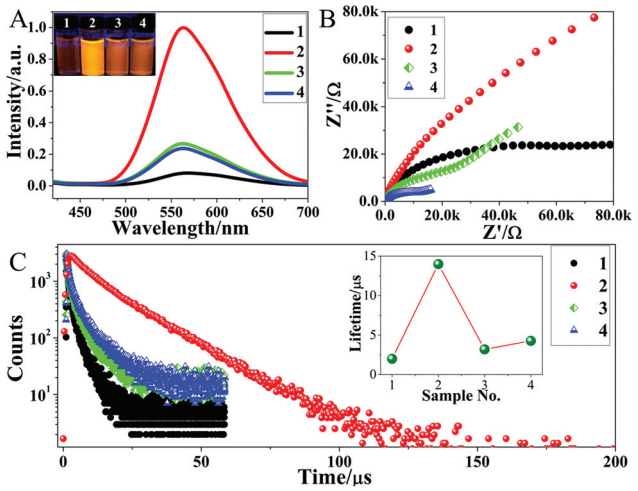

Fig. 3 (A) Fluorescence emission spectra, (B) Nyquist plots of electrochemical impedance spectroscopy, and (C) typical fluorescence decay curves for: (1) pristine Au NCs, (2) Au NCs/MgAl-ELDH, (3) Au NCs/CoAl-ELDH, (4) and Au NCs/CoNi-ELDH, respectively. The inset in A shows the digital photos of these samples under UV light irradiation.

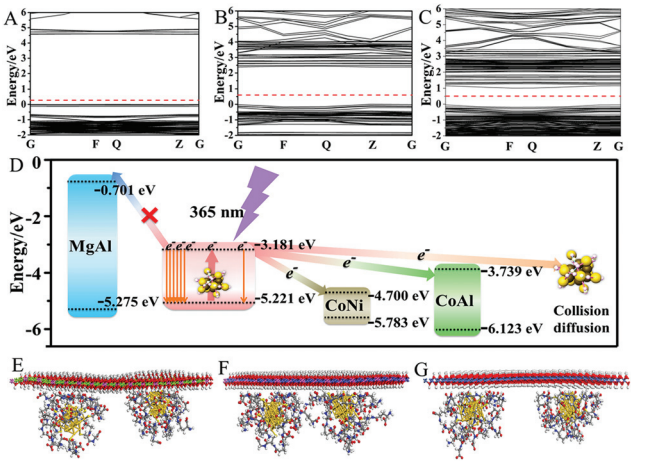

Fig. 4 Band structures of (A) MgAl-LDH, (B) CoAl-LDH, (C) CoNi-LDH, where the red dashed line represents the Fermi level. (D) The band edge placement of MgAl-LDH, CoAl-LDH, CoNi-LDH and Au NCs. The snapshot of (E) Au NCs/MgAl-ELDH, (F) Au NCs/CoAl-ELDH and (G) Au NCs/CoNi-ELDH after five nanoseconds of molecular dynamics simulation. Color denotation: red for O, white for H, dark blue for N, golden for Au, grey for C, yellow for S, green for Mg, pink for Al, blue for Co, and cyan for Ni.

This journal is © The Royal Society of Chemistry 2016

MgAl-ELDH, CoAl-ELDH, CoNi-ELDH are 77.65 eV, 43.95 eV and 35.43 eV, respectively, indicating the most stable structure of Au NCs/MgAl-ELDH.

In vitro fluorescence imaging performance and stability

The largely promoted fluorescence performances of Au NCs/ELDH are beneficial to the application of Au NCs in bio-imaging and cell labeling. The biocompatibility was firstly evaluated by studying the viability of HeLa cells incubated with pristine Au NCs, LDH support and Au NCs/ELDH for 24 h using the 3-(4,5-dimethylthiazol-2-yl)-3,5-diphenyltetrazolium bromide (MTT) method. As shown in Fig. 5A, cell viability for pristine LDH, Au NCs and Au NCs/ELDH remains 96.7%, 94.5% and 88.5% with the concentration as high as 100 g mL^{-1}, indicating the good biocompatibility and weak cytotoxicity of Au NCs and Au NCs/ELDH. Bio-imaging results (Fig. S14†) show that HeLa cells incubated with Au NCs or Au NCs/ELDH maintain good activity and normal morphology in the concentration range 6.25–100 g mL^{-1}; and the latter system exhibits a largely enhanced image resolution (Fig. 5B and S14†). Moreover, the average pixels of imaging zones can be calculated by using a confocal fluorescence microscope, and the fluorescence intensity of Au NCs/ELDH in the cytoplasm is much stronger than that of Au NCs with the concentration from 6.25 to 100 g mL^{-1}. Typically, the fluorescence intensity of Au NCs/ELDH is 7.21-fold stronger than that of pristine Au NCs (184.5 vs. 25.6) with the concentration of 100 g mL^{-1} (Fig. S15†), exhibiting a prominently enhanced imaging performance of Au NCs/ELDH.

Photostability, which is conducive to cell and tissue labeling, is an extremely important factor to develop Au NC-based bio-imaging agents.[21] As we know, Au NCs possess excellent photostability and anti-photobleaching properties in aqueous solutions, but its stability in cell culture has not been investigated so far. Fig. 5C shows the fluorescence emission intensity changes of Au NCs and Au NCs/ELDH in the cytoplasm of HeLa cells, and typical pictures are captured at a specific time point. The fluorescence intensity of Au NCs decreases rapidly and quenches within 4 min of continuous exciting light irradiation (Fig. 5C1 and S16A†). In contrast, the sample of Au NCs/ELDH undergoes a slight decrease in fluorescence intensity, and the cell morphology can be clearly observed even after 10 min of continuous irradiation and capturing (Fig. 5C2 and S16B†). The promoted anti-bleaching performances can be attributed to the localization of Au NCs on ELDH and the confinement e ect induced by ELDH nanosheets. Therefore, the Au NC/ELDH serves as a bio-imaging agent with good photostability in the microenvironment of the cytoplasm, which could be used for long-time bio-imaging and real-time dynamically monitoring of cell evolution.

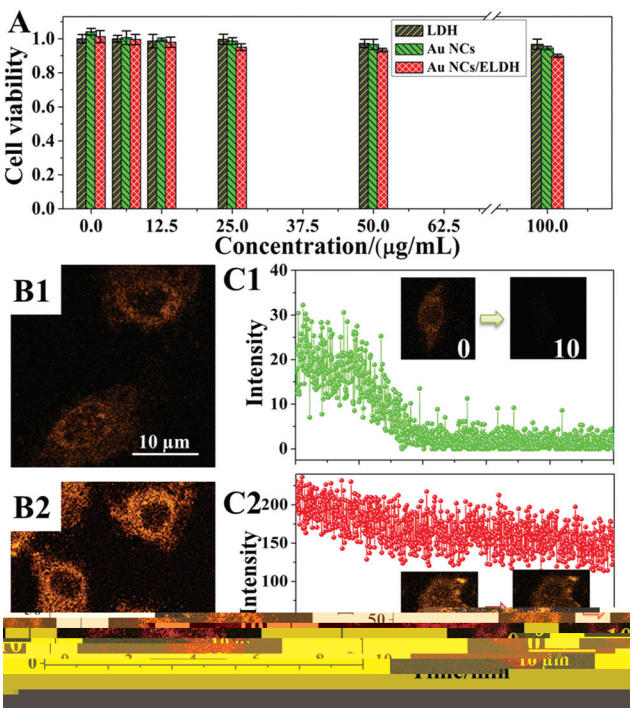

Fig. 5 (A) Viability of HeLa cells after 24 h incubation with different concentrations of LDH (black), Au NCs (green) and the Au NC/ELDH hybrid material (red). Confocal fluorescence images of HeLa cells incubated with (B1) pristine Au NCs and (B2) Au NCs/ELDH (100 μg mL^{-1}) for 24 h. Stability of (C1) Au NCs and (C2) Au NCs/ELDH in the cytoplasm of HeLa cells (the inset shows the sample photographs at 0 and 10 min).

Conclusions

In summary, we report a nano-hybrid material fabricated by Au NCs anchoring onto the surface of ELDH nanosheets, which exhibits high brightness, significantly promoted QY and excellent stability. MgAl-ELDH nanosheets impose a strong confinement e ect toward excited electrons of Au NCs, which inhibits the electron transfer, facilitates the electron/hole recombination and results in a largely enhanced fluorescence QY. DFT+U simulation confirms that excited electrons/holes of Au NCs are e ectively confined by MgAl-ELDH, leading to boosted fluorescence performance. The as-synthesized Au NC/ELDH material exhibits a distinct bio-imaging e ect and good stability in the cell microenvironment. Further studies on drug delivery for targeted diagnosis and therapy is in progress. Therefore, this work demonstrates a successful paradigm for the design and fabrication of inorganic–inorganic hybrid materials by virtue of the surface-confined emission enhancement imposed by a 2D ultrathin matrix, which serve as a promising candidate in bioimaging and cell labeling.

Acknowledgements

This work was supported by the National Natural Science Foundation of China (NSFC), the 973 Program (Grant No. 2014CB932104). M. Wei particularly appreciates the financial aid from the China National Funds for Distinguished Young Scientists of the NSFC. We acknowledge National Supercomputing Center in Shenzhen for providing the compu-

19 (a) X. Wen, P. Yu, Y. R. Toh, Y. C. Lee, K. Y. Huang, S. Huang, S. Shrestha, G. Conibeer and J. Tang, J. Mater. Chem. C, 2014, 2, 3826–3834; (b) P. Yu, X. Wen, Y. R. Toh, X. Ma and J. Tang, Part. Part. Syst. Charact., 2015, 32, 142–163.

20 (a) J. F. Zang, S. J. Bao, C. M. Li, H. J. Bian, X. Q. Cui, Q. L. Bao, C. Q. Sun, J. Guo and K. R. Lian, J. Phys. Chem. C, 2008, 112, 14843–14850; (b) A. D. Fabio, A. Giorgi, M. Mastragostino and F. J. Soavi, Electrochem. Soc., 2001, 148, A845–A850.

21 (a) Y. Yang, Q. Zhao, W. Feng and F. Li, Chem. Rev., 2013, 113, 192–270; (b) Y. Zhu, Z. Li, M. Chen, H. M. Cooper, G. Q. Lu and Z. P. Xu, Chem. Mater., 2012, 24, 421–423; (c) S. B. Lakshmanan, X. Zou, M. Hossu, L. Ma, C. Yang and W. J. Chen, Biomed. Nanotechnol., 2012, 8, 883–890.

This journal is © The Royal Society of Chemistry 2016